ENVIRONMENTAL RESEARCH
LETTERS

LETTER

Anthropogenic drivers of the accelerated decline in surface NO_2 over China during 2015–2022

Minglong Tang[1,2], **Ke Li**[1,2,*], **Zhenze Liu**[2], **Xi Chen**[2], **Yufen Wang**[2], **Jianbing Jin**[1,2], **Lei Chen**[2] and **Hong Liao**[1,2]

[1] State Key Laboratory of Climate System Prediction and Risk Management, Jiangsu Key Laboratory of Atmospheric Environment Monitoring and Pollution Control, Jiangsu Collaborative Innovation Centre of Atmospheric Environment and Equipment Technology, Joint International Research Laboratory of Climate and Environment Change, Nanjing University of Information Science and Technology, Nanjing, People's Republic of China
[2] School of Environmental Science and Engineering, Nanjing University of Information Science and Technology, Nanjing, People's Republic of China
* Author to whom any correspondence should be addressed.

E-mail: keli@nuist.edu.cn

Keywords: surface No_2, air pollutant trends, anthropogenic emissions, source sectors, meteorological influence

Supplementary material for this article is available online

OPEN ACCESS

RECEIVED
29 July 2025

REVISED
21 January 2026

ACCEPTED FOR PUBLICATION
12 February 2026

PUBLISHED
3 March 2026

Abstract

China has experienced accelerated decline in surface NO_2 concentrations under the condition of steady reduction in NO_x emissions over the past decade, but the reasons for such a nonlinear response in the changes of surface NO_2 to reduction in NO_x emissions remain unexplored. Through integration of measurements, a chemical transport model (GEOS-Chem), and a random forest (RF) model, we comprehensively quantified the contributions of emissions, meteorology, and chemical transformation to the observed trend in surface NO_2 during 2015–2022. After removing meteorological influences using the RF model, the anthropogenically-driven tendency was estimated to be -0.36 ppb y^{-1} for 2015–2018 (observed tendency: -0.09 ppb y^{-1}) and -1.23 ppb y^{-1} for 2019–2022 (observed tendency: -1.00 ppb y^{-1}), confirming the dominant role of anthropogenic drivers. Supported by long-term satellite measurements and GEOS-Chem model sensitivity simulations, we attributed this accelerated decline in surface NO_2 to the shift in emission sectors from power plants to transportation and industry after 2018. In addition to emissions, we demonstrated that the increased atmospheric oxidation capacity (i.e. higher ozone) played a key role in shifting NO_2 production from ozone-limited to NO-limited conditions, thereby making NO_2 concentration more sensitive to NO_x emission reductions. Further, measurement interference from oxidized nitrogen species for observing NO_2 can also contribute to the observed decline in surface NO_2, and its contribution doubled from 2015–2018–2019–2022. Our results elucidate the nonlinear response of the trend in surface NO_2 to reduction in NO_x emissions, and highlight the importance of understanding rapid changes in sectoral emissions and the chemical radicals in relation to future NO_2 controls.

1. Introduction

Air pollution is a major threat that greatly affects human health globally (Murray *et al* 2020, Xu *et al* 2023). As a typical urban pollutant, NO_2 is not only an important precursor of O_3 and $PM_{2.5}$, but also has substantial impacts on public health (Sun *et al* 2019, Copat *et al* 2020, Shen *et al* 2021, Xue *et al* 2023). Urban surface NO_2 is derived mainly from the combustion of fossil fuels by automobiles, industrial sectors, and thermal power plants. In 2021, the World Health Organization (WHO) proposed new air quality guidelines (Carvalho 2021, Kan 2022), which suggested that the annual average standard for surface NO_2 concentration should be reduced from 40 to 10 $\mu g\ m^{-3}$ (1 ppb = 1.88 $\mu g\ m^{-3}$ under 298 K and 1013 hPa). According to WHO data, in 2022, 77% of the population of 4000 cities in 74 countries was

exposed to an annual average concentration of surface NO_2 above this new standard (WHO 2021). Thus, this revision represents a substantial challenge in relation to controlling surface NO_2 pollution.

China is one of the countries exposed to the highest surface NO_2 concentration. In 2022, China's annual NO_2 concentration nationally was 12 ppb, and the city-level highest annual concentration was up to 21 ppb, much higher than the 2021 WHO standard. In fact, the Chinese government has implemented strict air pollution controls since 2013, and national NO_x emissions declined steadily by 21% during 2013–2017 and by 14% during 2018–2022. However, the observed concentrations of surface NO_2 in China did not decease correspondingly. For example, the observed change in surface NO_2 concentration between 2015 and 2018 was almost flat (Shen *et al* 2021, Li *et al* 2021b) and even increased by 3.5% during 2015–2017 on a national basis (Fan *et al* 2020). This demonstrates the complexity of the response in the trend of surface NO_2 concentration to reduction in NO_x emissions, which could be related to the interplay between pollutant emissions, meteorology, and chemical transformations within the atmosphere.

The concurrent rapid decline in NO_x emissions and surface NO_2 concentration following the COVID-19 lockdown serves as an example. Previous studies analyzed the changes in surface NO_2 during the period of the pandemic, and found that the remarkable decline in surface NO_2 concentrations in urban areas could be attributed predominantly to the ramping down of human activities while meteorology continued to affect the variation in concentration (e.g. Zhao *et al* 2020, Chu *et al* 2021, Hua *et al* 2021). These quantifications can be enabled by taking advantage of three-dimensional chemical transport models (e.g. GEOS-Chem) and machine learning models (e.g. random forest; RF) to separate anthropogenically-driven and meteorologically-driven contributions to the decline in NO_2 following the lockdown (Shi *et al* 2021, Guo *et al* 2022, Colombi *et al* 2023). The complex changes in air quality during the time of the COVID-19 pandemic highlight the importance of disentangling meteorologically-driven variability from the observed concentrations for short-term variability (Kroll *et al* 2020), but it is also important for long-term trends.

Previous studies on decadal-scale trends of NO_2 in China focused mainly on national changes in concentration, health impact assessments, and attribution of trends to anthropogenic emissions and meteorology (Lin *et al* 2021, Huang *et al* 2023, Xue *et al* 2023). For example, Qian *et al* (2023) used machine learning to analyze the changes in surface NO_2 concentrations during 2015–2022, and identified that anthropogenic emissions dominated the overall decline in surface NO_2. However, it failed to further quantify the role of multiple anthropogenic factors in driving the trend in surface NO_2, in particular its nonlinear response to continuous reduction in NO_x emissions from a decadal perspective (Fan *et al* 2020, Gao *et al* 2023, He *et al* 2017, Lin *et al* 2021, Li *et al* 2022a, Shen *et al* 2023, 2021). This is critical because ground-based observation sites in China are predominantly located around urban areas and sectoral contributions to NO_x emissions have changed substantially over the past decade. Thus, it remains unclear how such a transition might have already affected the observed trend in surface NO_2 concentrations.

In this study, we analyzed the spatiotemporal variation in observed NO_2 concentration in China over the past decade, and identified the driving factors of the NO_2 trends using the chemical transport model (GEOS-Chem) and the RF machine learning method. After separating the meteorological influence from observed NO_2 changes, we determined that there was accelerated decline in the anthropogenically-driven NO_2 after 2018 while NO_x emissions decreased steadily. This nonlinear response in the trend of surface NO_2 concentrations to reduction in NO_x emissions was further attributed to a shift in sectoral emission reductions, as well as the rapid changing of chemical radicals.

2. Materials and methods

2.1. NO_2 measurements

Data of hourly observations of surface NO_2 concentration at ~360 cities across China during 2015–2022 were obtained from the China environmental monitoring platform (https://air.cnemc.cn:18007/), which forms part of the routine monitoring of urban air quality in China. Satellite-derived NO_2 column data have been used widely to evaluate changes in NO_x emissions (Lamsal *et al* 2011, Liu *et al* 2017, Shah *et al* 2020). In this study, we used monthly tropospheric NO_2 column data from the OMI instrument with spatial resolution of $0.25° \times 0.25°$ (see supplementary material).

2.2. RF model

The RF model has better performance than traditional statistical models in meteorological normalization (Grange *et al* 2018). In recent years, many studies have employed the RF method to separate the effects of meteorological conditions and anthropogenic emissions in relation to variations in air pollutants (e.g. Shi *et al* 2021, Guo *et al* 2022, Colombi *et al* 2023). In this study, the RF model was developed for each city based on eight predictors: three time variables (day of the week, day of the year, and Unix time) to represent anthropogenic emission changes and five key meteorological variables (surface temperature, wind speed, wind direction, relative humidity, and boundary layer height) (see table S1). These

five meteorological variables have been widely adopted in previous studies to capture the NO_2 variations using the RF model (e.g. Shi *et al* 2021, Li *et al* 2022b, Schatke *et al* 2022, Wei *et al* 2022). The training dataset comprised 80% of the dataset, and the remaining 20% was reserved for evaluation.

To remove the meteorological influence on observed NO_2 trends at each city, after the RF model was trained for each city, we performed 1000 resamplings to construct a new dataset of predictor features, including time variables (but not the Unix time) and meteorological variables from the original dataset. For each resampled dataset, daily NO_2 concentrations were predicted using the city-specific RF model. The 1000 predicted values were then averaged to represent NO_2 concentrations under 'average' meteorological conditions for 2015–2022. This procedure was applied to every city and every day from 2015 to 2022, and the resulting meteorology-normalized NO_2 concentrations were used to recalculate the 2015–2022 NO_2 trends, which we interpret as anthropogenically-driven trends (see supplementary material).

2.3. GEOS-Chem model

Changes in surface NO_2 concentration in China during 2015–2022 were simulated using the GEOS-Chem model (version 13.3.3; https://geoschem.github.io) driven by the GEOS-5 forward processing (GEOS-FP) meteorological reanalysis. The model combines complex O_3–NO_x–VOC–aerosol–halogen tropospheric chemistry. Model simulations were performed over a nested domain (15°–55°N, 90°–135°E) with horizontal resolution of 0.25° × 0.3125° and 47 vertical layers. The chemical boundary conditions were provided every 3 h by a global GEOS-Chem simulation with resolution of 4° × 5 °.

The monthly sectoral anthropogenic emissions for China were taken from the MEIC inventory developed by Tsinghua University (http://meicmodel.org.cn/). Given that data in this inventory up until only 2020 are publicly available, anthropogenic emissions of NO_x and VOCs for 2021 and 2022 were estimated using data reported by the Ministry of Ecology and Environment (table S2). It should be noted that the scaling factors adopted in this study were highly consistent with the reported TROPOMI-constrained NO_x emission reduction of 13% during 2019–2022 (Li *et al* 2024). The configuration for natural NO_x emissions, including lighting NO_x and soil NO_x emissions are calculated on the basis of the assimilated GEOS-FP meteorology.

In this study, we performed two sets of multi-year simulation experiments using the high-resolution GEOS-Chem model of 0.25° × 0.3125°, as detailed in table S3. Observed national NO_2 levels are the highest of 16.5 ppb in January and the lowest of 7.4 ppb in July in 2022. To save computational resources, we use January and July to represent the different pollution levels of NO_2 over China. The model experiments are detailed as follows:

(1) To quantify the effects of changes in anthropogenic emissions, we conducted separate 8 year model simulations (2015–2022) for both January and July. All the runs were performed with fixed meteorology for 2015 but varying anthropogenic emissions.
(2) To explore the impact of reductions in emissions by different sectors on surface NO_2 concentrations, we conducted the baseline 2015 (2019) simulation and perturbation simulations in which sectoral NO_x emissions from power plant, industry, and transportation were respectively reduced to reflect their changes during 2015–2018 (2019–2022). Emissions of NO_x by the residential sector are low and were not perturbated in the experiments.

3. Results and discussion

3.1. Observed accelerated decline in surface NO_2 concentrations during 2015–2022

We focused on the four major urban agglomerations in China: the North China Plain (NCP; 35°–40°N, 114°–118°E), Yangtze River Delta (YRD; 30°–33°N, 119°–122°E), Pearl River Delta (PRD; 21.5°–24°N, 112°–115.5°E), and Sichuan Basin (SCB; 28.5°–31.5°N, 103.5°–107°E). During 2015–2018, the SCB region recorded the highest annual average NO_2 concentration of 38 ppb, followed by the PRD (32 ppb), the NCP (31 ppb), and the YRD (22 ppb). During 2019–2022, surface NO_2 concentration in China declined quickly. By 2022, the annual NO_2 concentration had reduced to 27, 22, 20, and 14 ppb in the SCB, PRD, NCP, and YRD, respectively (figures S2 and S3). These widespread reductions in annual NO_2 concentration suggest remarkable improvement in NO_2 pollution across China.

The spatial distributions of the observed NO_2 tendencies in the two periods during 2015–2022 are shown in figures 1(a) and (b). The magnitude of the overall tendency in surface NO_2 concentration in China during 2015–2018 was only -0.09 ppb y^{-1}, and the small scale of this tendency is attributed mainly to the strong regional heterogeneity in the NO_2 tendency. For example, the NO_2 concentration declined by -0.73 ppb y^{-1} in the NCP, but increased by 0.35 and 0.37 ppb y^{-1} in the PRD and SCB, respectively. In contrast, during 2019–2022, there was extensive decline in the NO_2 concentration across the country, leading to an accelerated rate of reduction in the overall tendency of -1.00 ppb y^{-1} nationally. It should be noted that we excluded data from January–February 2020 in the calculation of the NO_2 tendency to minimize the impact of the COVID-19 pandemic. Seasonally, surface NO_2 concentration during 2019–2022 exhibited the fastest rate of decline

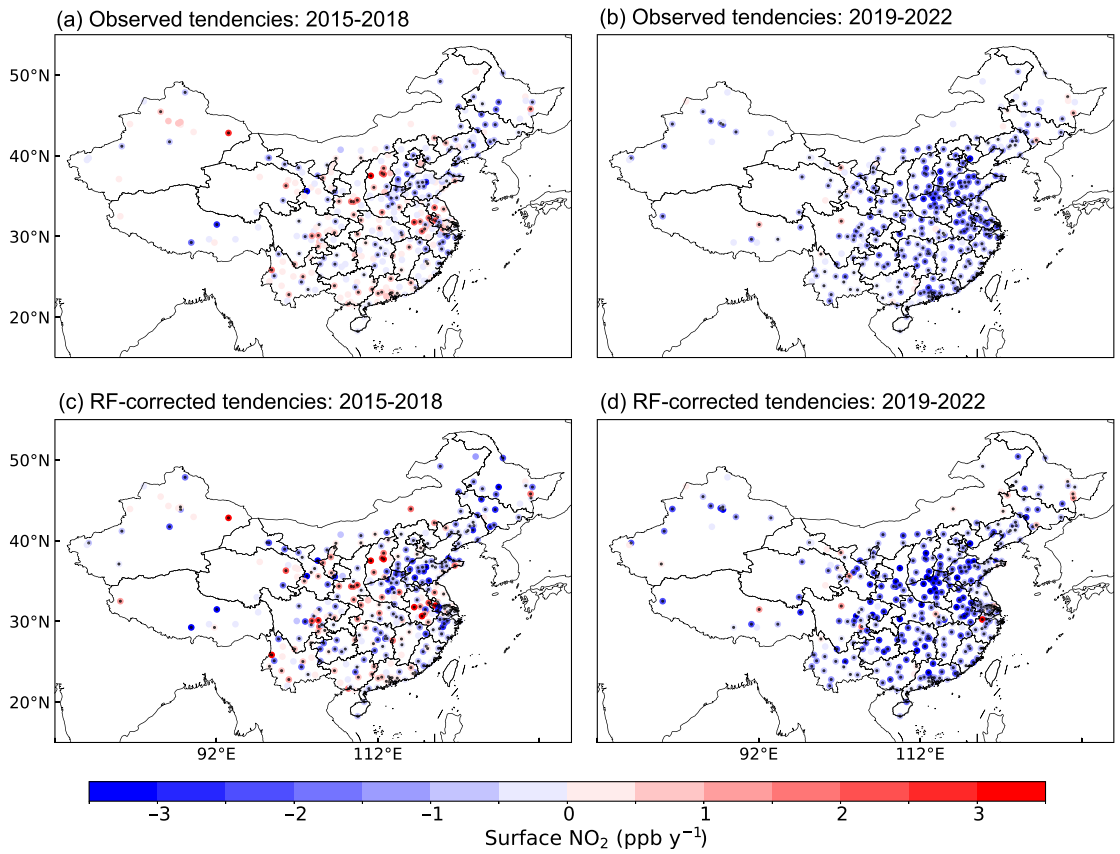

Figure 1. Observed and RF-corrected tendencies in surface NO_2 concentration (ppb y^{-1}) during 2015–2022. The RF-corrected tendencies were estimated using the RF model to remove the effects of meteorology. (a) and (b) Observed tendencies in NO_2 concentration during 2015–2018 and 2019–2022, respectively. (c) and (d) RF-corrected tendencies in NO_2 concentration during 2015–2018 and 2019–2022, respectively. Black dots indicate estimated tendencies that are statistically significant above the 95% confidence level. It should be noted that NO_2 data for January–February 2020 was removed to eliminate the impact of the COVID-19 pandemic.

in autumn (-1.15 ppb y^{-1}), followed by winter (-0.94 ppb y^{-1}), spring (-0.86 ppb y^{-1}), and summer (-0.76 ppb y^{-1}). It demonstrates that the accelerated rate of decline in surface NO_2 concentration during 2019–2022 had no obvious seasonal difference (figure S4).

Considering that meteorology might play a role in the spatial and temporal differences of NO_2 tendencies, the next section separates the role of anthropogenic emissions and meteorology in the observed NO_2 tendencies using both machine learning and chemical transport modeling approaches.

3.2. Anthropogenic contributions to observed NO_2 tendencies

The tendencies of the surface NO_2 concentration after removing meteorological influences using the RF model (see section 2.2) are shown in figures 1(c) and (d), which can be treated as the anthropogenically-driven tendency. During 2015–2018, the anthropogenically-driven tendency was estimated as -0.36 ppb y^{-1} and it increased to -1.23 ppb y^{-1} during 2019–2022. It indicates that anthropogenic emissions were the dominant factor driving the reduction in NO_2 concentration in both two periods, while meteorological factors were unfavorable for supporting the decline in NO_2. Spatially, during 2019–2022, the contribution of anthropogenic emissions to the observed tendency was close to 100% in the NCP (102%) and PRD (106%), suggesting a very minor contribution from meteorology. However, meteorological conditions were conducive to the reduction in NO_2 in the YRD (anthropogenic contribution: 54%) but unfavorable in the SCB region. Thus, after isolating the influence of meteorology in the observed NO_2 tendencies, we still found that the accelerated rate of reduction in NO_2 during 2019–2022 can be attributed to anthropogenic drivers.

Next, we conducted simulations for 2015–2022 using the nested GEOS-Chem model with the fixed meteorological conditions of 2015. The model shows that the NO_2 change in January (July) during 2015–2018 was 0% (3.7%), while there was notable reduction of -9.8% (-13%) in January (July) during 2019–2022 (figure 2). For comparison, the RF model also shows rapid decline in NO_2 of -11.4% (-17.5%) in January (July) during 2019–2022, and that the

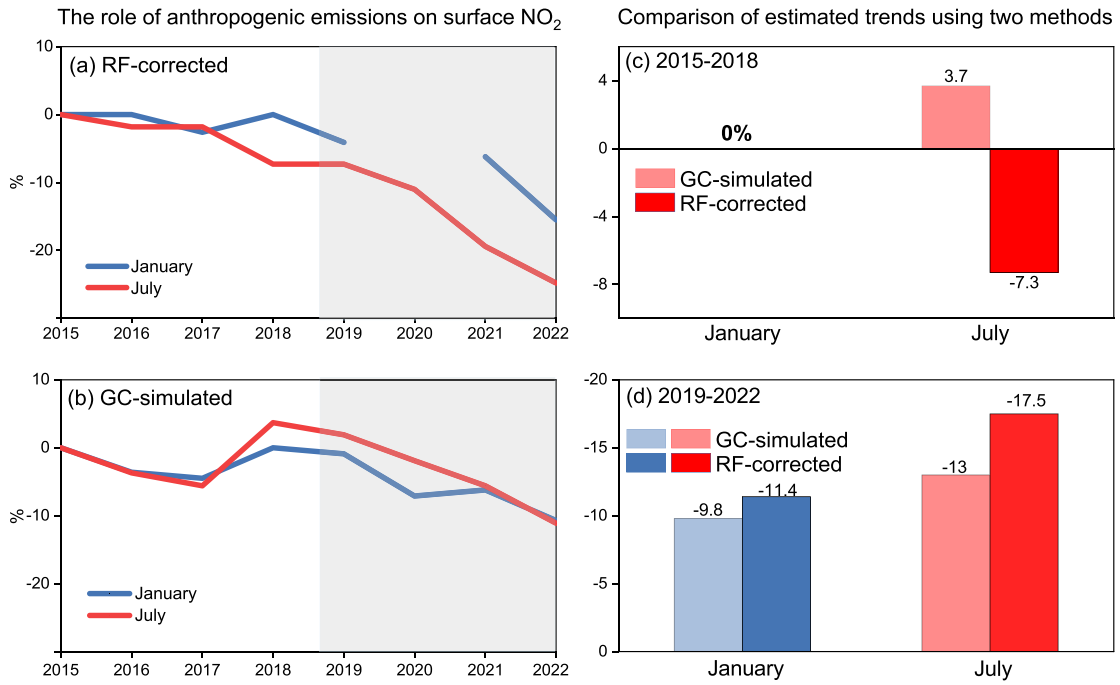

Figure 2. The GEOS-Chem-simulated changes in NO_2 during 2015–2022 with fixed meteorology and their comparison with the RF-corrected NO_2. (*Left*) Using the RF and GEOS-Chem methods, the simulated changes (unit: %) in NO_2 in January (blue) and July (red) relative to 2015 were driven by emission changes during 2015–2022 but with the fixed meteorological conditions of 2015. (*Right*) Comparison of surface NO_2 percentage changes between the GEOS-Chem-modeled and RF-corrected values during 2015–2022.

change in NO_2 during 2015–2018 was small. While the RF-corrected NO_2 decline (−7.3%) in July during 2015–2018 also suggests a declining tendency, this is not captured by the GEOS-Chem model. This model-observation discrepancy may be attributed to the strong spatial heterogeneity in NO_x emission changes over 2015–2018, which makes the GEOS-Chem model difficulty in simulating the observed city-level NO_2 changes. The very short lifetime of NO_x in summer (Shah *et al* 2020) can also results in a worse model performance in this season. Overall, the RF and GEOS-Chem models demonstrate reasonable consistency in the overall declines (particularly for 2019–2022) in NO_2, confirming that changes in anthropogenic emissions were the main driver of the rapid decline in NO_2 during 2019–2022.

Furthermore, we compared the anthropogenically-driven tendencies in NO_2 in January and July during 2015–2022, as estimated by the GEOS-Chem and RF models. For the period of rapid decline in surface NO_2 during 2019–2022, it is evident that the GEOS-Chem model driven by fixed meteorology reproduces the RF-corrected NO_2 decline by 86% and 74% in January and July, respectively (figure 2). It demonstrates the strong capability of the GEOS-Chem model in capturing the response of surface NO_2 concentration to reduction in NO_x emissions. Thus, we took advantage of the skill of this model to further elucidate the anthropogenic drivers by conducting a set of sensitivity experiments, as discussed in the following sections.

3.3. Satellite and modeling evidence of shifting contributions of sectoral emissions

The magnitudes of the reduction in NO_x emissions by 2.8 Tg during 2015–2018 and by 2.6 Tg during 2019–2022 are similar (figure S1), but there is marked inconsistency with the associated tendency in surface NO_2. Based on the changes in NO_x emissions by different source sectors obtained from the MEIC inventory, we found that NO_x reductions during 2015–2018 were contributed predominantly by power plants, but subsequent NO_x emission controls shifted toward the transportation and industry sectors (Li *et al* 2024). To verify this shift in sectoral emissions, we selected the NCP region as an example case.

We took the three power plant grid points with the largest emissions in the NCP region (results were similar when 5 or 10 grid points were selected) to focus on their changes in the bottom-up emissions and satellite NO_2 columns. Similar results can be also found for other regions (such as the YRD) where power plant emissions are much smaller than those in the NCP region (figure S5). In contrast, we selected the four provincial capital cities in the NCP region (i.e. Beijing, Shijiazhuang, Tianjin, and Jinan) to show the NO_2 changes at the surface and derived from space that would be affected mainly by transportation and industrial sources.

Figure 3 shows that along with the rapid reductions in power plant emissions during 2015–2018, the satellite NO_2 columns for the corresponding grid cells also declined substantially, whereas both the surface

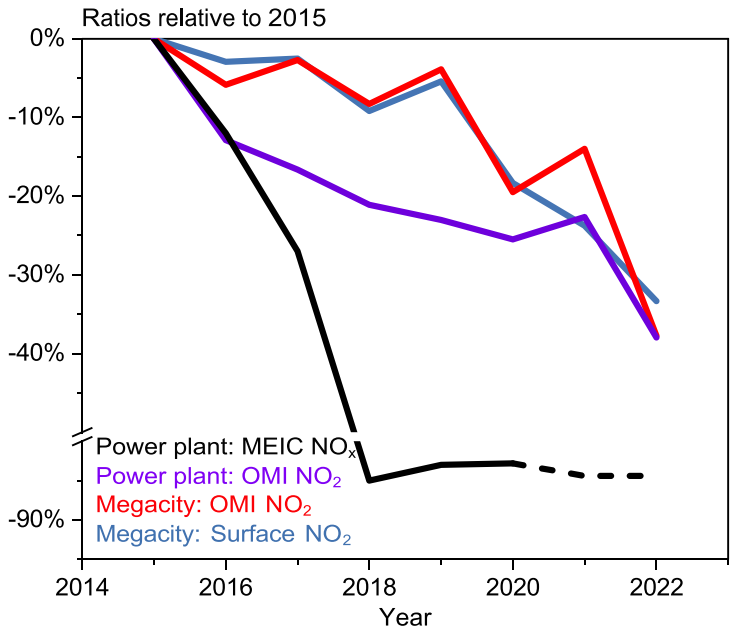

Figure 3. Satellite evidence of shifting sectoral contribution to NO_x reductions. Time series of observed annual mean quantities (values are presented as ratios relative to 2015) averaged over the NCP: surface NO_2 (blue, solid) and OMI NO_2 columns (red, solid) for the four provincial capital cities (i.e. Beijing, Shijiazhuang, Tianjin, and Jinan) are used to represent the changes from megacity. MEIC NO_x emissions (black, solid) and corresponding OMI NO_2 columns (dark red, solid) at the three grid cells with the highest MEIC NO_x emissions from power plant in the NCP region are used to represent the changes from power plant sector. Dashed back line shows the relative changes in power plant NO_x emissions inferred by a top-down method (Li *et al* 2024). It should be noted that the results were similar for changes in power plant emissions if the top 5 or 10 grid points were selected.

NO_2 concentrations and the satellite-derived NO_2 columns for the provincial cities exhibited only small reduction. After 2018, in contrast, there was rapid and continuous decline in the observed NO_2 values at the surface and from derived from satellite over these provincial cities. The flat satellite-derived NO_2 columns over the power plant grid cells are consistent with the reported sectoral emission changes from the bottom–up inventory. The different trends from the satellite observations suggest a clear shift in NO_x emission controls from power plants to other anthropogenic sources after 2018.

Such a shift in sectoral reductions could be important in explaining the diverse tendencies in observed NO_2. On the one hand, this is because power plants are generally located far from urban observation sites, and the lifetime of NO_2 (a few hours with smearing distances of less than 100 km) is too short for it to be dispersed from power plants to urban regions. On the other hand, power plants are mainly located in northern China and their impacts on the tendency of NO_2 nationally should be limited. Therefore, the rapid reductions in power plant emissions before 2018 had less impact on the observed urban NO_2 concentrations, and the subsequent decline in surface NO_2 concentrations could have been driven mainly by urban transportation and industrial controls.

To further demonstrate the dependence of urban NO_2 concentrations on different sectoral emissions, we conducted model sensitivity simulations by perturbing NO_x reductions in different sectors. Figure 4(S6) show the simulated impact of reductions in sectoral emissions on the percentage changes in surface NO_2 in different periods during 2015–2022 in July and January, respectively. It is evident that during 2015–2018, emission changes of power plants, industry, and transportation led to changes of −2.6% (−2.1%), 2.0% (3.7%), and 0.5% (0.9%) in NO_2 in July (January), respectively. This sectoral offset resulted in small changes in the tendency of surface NO_2 during 2015–2018. During 2019–2022, the accelerated rate of decline in NO_2 can be attributed mainly to the impact of reductions in the emissions of industry and transportation. During 2019–2022, decline in the emissions of power plants, industry, and transportation reduced surface NO_2 concentrations by −0.1% (−1.5%), −4.1% (−7.1%), and −4.4% (−6.3%) in July (January), respectively. Overall, our sensitivity modeling with sectoral emission perturbations further clarifies the individual role of the emissions of different sectors on the tendency of urban NO_2 concentrations.

3.4. Role of changing chemical radicals in accelerated NO_2 tendencies

In addition to emissions, the surface NO_2 concentration is also affected by chemical transformations within the atmosphere. Table S4 lists the major chemical sources and sinks of NO_2 in which chemical radicals could play an important role. Recent studies reported increased atmospheric oxidation capacity over

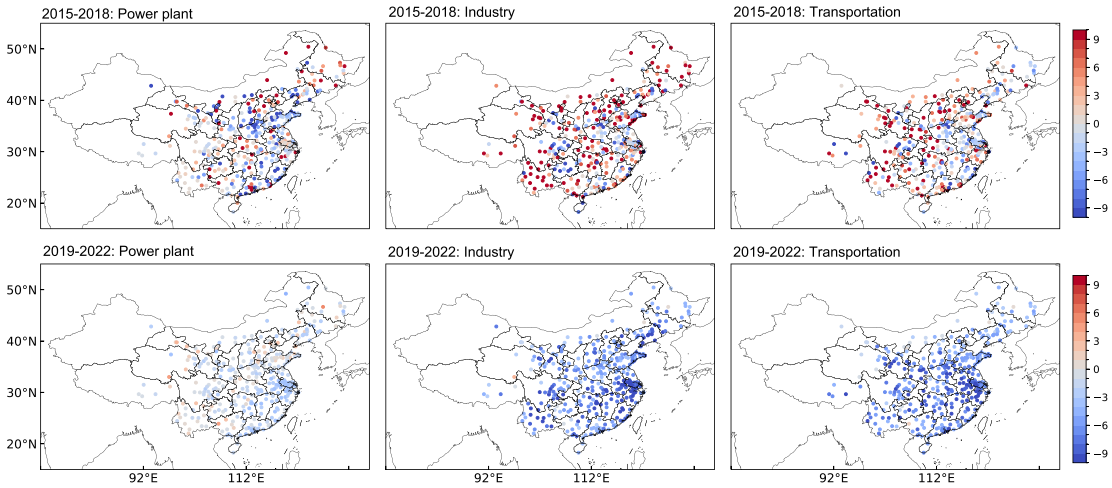

Figure 4. Simulated impact of reductions in sectoral NO_x emissions on the changes (unit: %) in surface NO_2 concentrations in July in two periods of 2015–2018 and 2019–2022. (*Top*) the results represent the differences between the baseline 2015 simulation and the perturbation simulations in which sectoral NO_x emissions from power plant, industry, and transportation were respectively reduced to reflect their changes during 2015–2018. (*Bottom*) similarly, but for the differences between the baseline 2019 simulation and the perturbation simulations with sectoral emission reduction during 2019–2022. Emissions of NO_x by the residential sector are low and were not considered here.

urban China after 2013 (Chen *et al* 2020, Fu *et al* 2020, Wang *et al* 2024), which enhanced the chemical production of airborne pollutants (e.g. nitrates). The following examines whether the observed NO_2 declines in China over the past decade were influenced by the changing chemical radicals in response to emission reductions.

To quantify changes in the NO_2 chemical budget in response to emission reductions, we archived the simulated reaction rates for all chemical sources and sinks of NO_2 (listed in table S4) at every GEOS-Chem time step. The relative importance of each reaction was then calculated as the ratio of its reaction rate to the total chemical sources or sinks of NO_2. Figure 5 shows the relative contributions of different chemical pathways to the total NO_2 budget within the boundary layer over the NCP during 2015–2018 and 2019–2022.

Firstly, the total rate of chemical reactions (K) declined notably by 11% during 2019–2022, and the decline was only 3% during 2015–2018, demonstrating that the change in the total rate of chemical reaction followed the change in the simulated NO_2 concentration during 2015–2022. The dominant pathway of NO_2 sources was O_3 + NO reaction, which is determined by the relative availability of O_3 and NO. By examining the ratio of NO_x–O_3, we find a remarkable decrease in the ratio of NO_x–O_3 during 2019–2022 in relative to 2015–2018 (figure S7), suggesting a clear shift from O_3-limited to NO-limited condition for the O_3 + NO reaction. Such a transition is more evident in January which is consistent with the stronger titration effect of O_3 by NO.

In addition to O_3, other chemical radical (e.g. NO_3) mainly played a role in summertime during 2015–2018. The NO_2 budget in July is more complex owing to the more active photochemistry in summer. The major chemical sources were O_3 + NO reaction and N_2O_5 decomposition, and the chemical sink reactions were dominated by NO_2 photolysis and NO_2 + NO_3 reaction. The relative contribution by NO_2 + NO_3 reaction to the total sink in July increased from 23.7% to 26.7%, suggesting increased contribution from NO_3 radicals. In contrast, during 2019–2022, there was almost no change (∼0.5%) in the relative importance of NO_2 + NO_3 reaction. These results highlight the important role of the changed atmospheric oxidation capacity in the observed NO_2 tendencies.

Furthermore, the observed NO_2 tendencies could also be affected the observation error that has been noted in previous work (Lamsal *et al* 2008, Liu *et al* 2018). NO_2 concentration from routine monitoring sites is observed through molybdenum-catalyzed conversion to nitric oxide and a subsequent chemiluminescence measurement, which could be interfered by other oxidized nitrogen species. Here, we took advantage of the GEOS-Chem simulated nitrogen species (i.e. NO_2, HNO_3, PAN, and all alkyl nitrates) to calculate correction factors for this observation error by introducing the summation of all alkyl nitrates, 95% of PAN, and 35% of HNO_3 (Lamsal *et al* 2008, Liu *et al* 2018). It means that changes in these reactive species over the past decade could have affected the observed NO_2 tendencies. Our calculation shows that this observation error could have contributed to reduction in the NO_2 tendencies by 4% (14%) in January (July) during 2015–2018, and 10% (29%) in January (July) during 2019–2022. Compared with January, this observation error

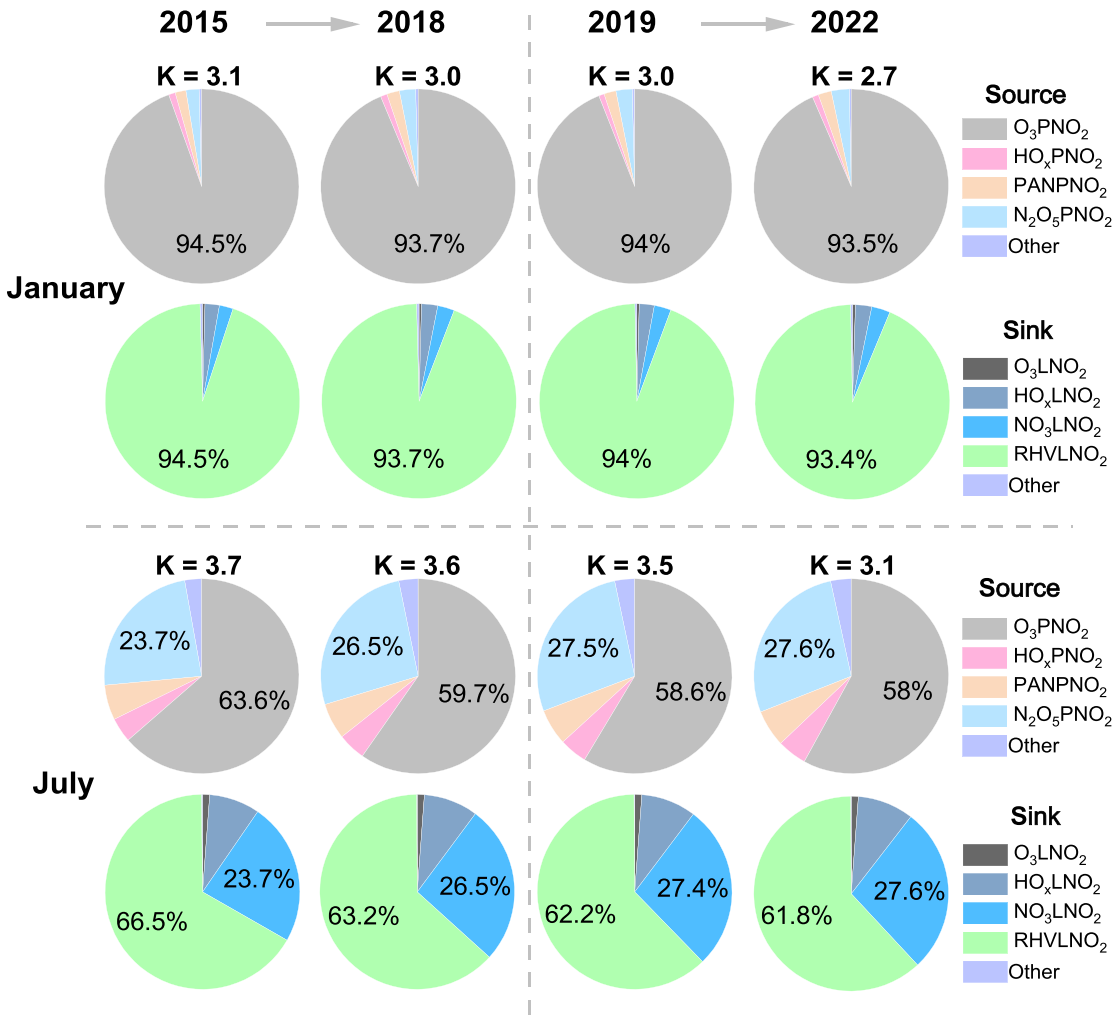

Figure 5. Simulated contributions of different chemical pathways to the total source and sink of NO_2 for the boundary layer over the North China Plain (NCP) during 2015–2022. (*Left to right*) Simulated contributions by different chemical reactions in 2015, 2018, 2019, and 2022, respectively. In the figure legend, the naming convention such as '$APNO_2$' means that NO_2 is produced by reaction with 'A'; '$ALNO_2$' means that NO_2 is consumed by reaction with 'A'; 'Others' represents the summation of the remaining reactions that are not listed here. All of the chemical source and sink reactions of NO_2 are listed in table S4. The K (unit: 10^8 molec cm^{-3} s^{-1}) means the total reaction rate of NO_2 production or consumption.

had greater impact in July owing to the faster production of reactive nitrogen species in summer. In short, measurement interference from oxidized nitrogen species played an important role in the decline in surface NO_2 concentration and its contribution doubled from 2015–2018–2019–2022.

4. Summary and policy implications

In this study, we analyzed the variation tendencies of surface NO_2 concentration in China across different periods during 2015–2022, and our results revealed notable acceleration in the observed decline in NO_2 from 2015–2018 (-0.09 ppb y^{-1}) to 2019–2022 (-1.00 ppb y^{-1}). After removing the meteorological influence using the RF model, the estimated anthropogenically-driven tendency was -0.36 and -1.23 ppb y^{-1} for 2015–2018 and 2019–2022, respectively, confirming the dominant role of anthropogenic emissions in driving the reduction in NO_2. We attributed this accelerated rate of decline in NO_2 to the shift in anthropogenic emission sectors from power plants to the transportation sector, supported by long-term satellite measurements and model sensitivity simulations. In addition to emissions, we found that increased O_3 played an important role in shifting the O_3 + NO reaction from O_3-limited condition to NO-limited condition, and NO_2 measurement interference from oxidized nitrogen species could also result in the declining of surface NO_2 and its contribution doubled from 2015–2018–2019–2022.

Our results identified the key emission sectors driving the accelerated rate of NO_2 decline. Considering that urban surface NO_2 is most responsive to changes in transportation sources, future prioritization of green transportation, e.g. promoting electric vehicles, improving the utilization rate of public transportation, and developing clean-energy transportation modes, will play a crucial role in further reducing NO_2 pollution. This has been demonstrated

by the concurrent decline in anthropogenic NO_x emissions and surface NO_2 concentrations during the COVID-19 lockdown (Le *et al* 2020, Liu *et al* 2020, Zhao *et al* 2020, Chu *et al* 2021, Li *et al* 2021a, Yang *et al* 2021).

With the introduction of new WHO air quality standards in 2021, the annual and daily NO_2 guidelines were updated to 10 and 25 μg m^{-3} (1 ppb = 1.88 μg m^{-3} under 298 K and 1013 hPa), respectively. However, in 2022, the annual NO_2 concentration in China's major urban agglomerations remained 2–3 times the WHO standard, and the average number of days on which the standard was exceeded was 100–200 among urban clusters. Even if the rate of decline in surface NO_2 concentrations observed during 2019–2022 could be maintained, it will still take approximately 10 years before the new WHO air quality standards are met, highlighting the importance of sustainable reductions in emission in the future.

In addition to strict emission controls, meteorological and chemical factors also affect the concentration of surface NO_2. For example, the observed NO_2 tendency during 2015–2018 was corrected from −0.09 to −0.36 ppb y^{-1} after the meteorological influence was removed, highlighting the important role of meteorology in affecting short-term NO_2 formation and dispersion. However, in the long term, changing chemical radicals in the process of emission reductions could play a more important role than meteorology in affecting the surface NO_2 tendency. Consequently, these factors should be considered when formulating future emission reduction strategies to ensure that long-term air quality improvement targets are achievable.

Acknowledgment

This work is supported by the National Key R&D Program of China (2022YFE0136100, 2024YFC3714200), the Jiangsu Carbon Peak and Neutrality Science and Technology Innovation fund (BK20220031), and the Jiangsu Science Fund for Distinguished Young Scholars (BK20240035). Zhenze Liu thanks the National Natural Science Foundation of China (42307140), the Natural Science Foundation of Jiangsu Province (SBK2023043946), and the China Postdoctoral Science Foundation for funding (2023M731749). We also thank for very valuable suggestions by Muhammad Imran Shahzad from COMSATS University Islamabad.

Data availability statement

The hourly surface NO_2 concentration data for China are archived at https://doi.org/10.5281/zenodo.16163974. The OMI NO_2 data were obtained from https://avdc.gsfc.nasa.gov/Data2/NO2TropCS30/global_1440x720/daily/ASCII/. The GEOS-Chem model code (version 13.3.3) is open-sourced at https://zenodo.org/records/5748260. The GEOS-FP meteorological reanalysis data are available from http://geoschemdata.wustl.edu/ExtData/GEOS_0.25x0.3125_AS/GEOS_FP/. The anthropogenic emission data for China (MEIC v1.4) are freely accessible from http://meicmodel.org.cn/?page_id=541&lang=en.

Supplementary Data available at http://doi.org/10.1088/1748-9326/ae452b/data1.

Conflict of interest

The authors declare that they have no conflict of interest.

Author contributions

Minglong Tang
Formal analysis (lead), Investigation (lead), Methodology (lead), Writing – original draft (lead)

Ke Li 0000-0002-9181-3562
Conceptualization (lead), Funding acquisition (lead), Investigation (equal), Writing – review & editing (lead)

Zhenze Liu
Funding acquisition (supporting), Methodology (supporting), Software (supporting)

Xi Chen 0000-0002-5987-1578
Visualization (supporting), Writing – review & editing (supporting)

Yufen Wang
Software (supporting)

Jianbing Jin
Writing – review & editing (supporting)

Lei Chen
Writing – review & editing (supporting)

Hong Liao
Supervision (supporting), Writing – review & editing (supporting)

References

Carvalho H 2021 New WHO global air quality guidelines: more pressure on nations to reduce air pollution levels *Lancet Planet. Health* **5** e760–e1

Chen S, Wang H, Lu K, Zeng L, Hu M and Zhang Y 2020 The trend of surface ozone in Beijing from 2013 to 2019: indications of the persisting strong atmospheric oxidation capacity *Atmos. Environ.* **242** 117801

Chu B, Zhang S, Liu J, Ma Q and He H 2021 Significant concurrent decrease in $PM_{2.5}$ and NO_2 concentrations in China during COVID-19 epidemic *J. Environ. Sci.* **99** 346–53

Colombi N K, Jacob D J, Yang L H, Zhai S, Shah V, Grange S K, Yantosca R M, Kim S and Liao H 2023 Why is ozone in South Korea and the Seoul Metropolitan Area so high and increasing? *Atmos. Chem. Phys.* **23** 4031–44

Copat C, Cristaldi A, Fiore M, Grasso A, Zuccarello P, Santo Signorelli S, Conti G O and Ferrante M 2020 The role of air pollution (PM and NO_2) in COVID-19 spread and lethality: a systematic review *Environ. Res. Lett.* **191** 110129

Fan H, Zhao C and Yang Y 2020 A comprehensive analysis of the spatio-temporal variation of urban air pollution in China during 2014–2018 *Atmos. Environ.* **220** 117066

Fu X, Wang T, Gao J, Wang P, Liu Y, Wang S, Zhao B and Xue L 2020 Persistent heavy winter nitrate pollution driven by increased photochemical oxidants in northern China *Environ. Sci.* **54** 3881–9

Gao C, Zhang F, Fang D, Wang Q and Liu M 2023 Spatial characteristics of change trends of air pollutants in Chinese urban areas during 2016–2020: the impact of air pollution controls and the COVID-19 pandemic *Atmos. Res.* **283** 106539

Grange S K, Carslaw D C, Lewis A C, Boleti E and Hueglin C 2018 Random forest meteorological normalisation models for Swiss PM10 trend analysis *Atmos. Chem. Phys.* **18** 6223–39

Guo Y, Li K, Zhao B, Shen J, Bloss W J, Azzi M and Zhang Y 2022 Evaluating the real changes of air quality due to clean air actions using a machine learning technique: results from 12 Chinese mega-cities during 2013–2020 *Chemosphere* **300** 134608

He J, Gong S, Yu Y, Yu L, Wu L, Mao H, Song C, Zhao S, Liu H and Li X 2017 Air pollution characteristics and their relation to meteorological conditions during 2014–2015 in major Chinese cities *Environ. Pollut.* **223** 484–96

Hua J, Zhang Y, de Foy B, Shang J, Schauer J J, Mei X, Sulaymon I D and Han T 2021 Quantitative estimation of meteorological impacts and the COVID-19 lockdown reductions on NO_2 and PM2. 5 over the Beijing area using generalized additive models (GAM) *J. Environ. Manage.* **291** 112676

Huang K, Zhu Q, Lu X, Gu D and Liu Y 2023 Satellite-based long-term spatiotemporal trends in ambient NO_2 concentrations and attributable health burdens in China from 2005 to 2020 *GeoHealth* **7** e2023GH000798

Kan H 2022 World Health Organization air quality guidelines 2021: implication for air pollution control and climate goal in China *Chin. Med. J.* **135** 513–5

Kroll J H, Heald C L, Cappa C D, Farmer D K, Fry J L, Murphy J G and Steiner A L 2020 The complex chemical effects of COVID-19 shutdowns on air quality *Nat. Chem.* **12** 777–9

Lamsal L, Martin R, Padmanabhan A, Van Donkelaar A, Zhang Q, Sioris C, Chance K, Kurosu T and Newchurch M 2011 Application of satellite observations for timely updates to global anthropogenic NO_x emission inventories *Geophys. Res. Lett.* **38** L05810

Lamsal L, Martin R, Van Donkelaar A, Steinbacher M, Celarier E, Bucsela E, Dunlea E and Pinto J 2008 Ground-level nitrogen dioxide concentrations inferred from the satellite-borne ozone monitoring instrument *J. Geophys. Res. Atmos.* **113** D16308

Le T, Wang Y, Liu L, Yang J, Yung Y L, Li G and Seinfeld J H 2020 Unexpected air pollution with marked emission reductions during the COVID-19 outbreak in China *Sci. Total Environ.* **369** 702–6

Li C, Hammer M S, Zheng B and Cohen R C 2022a Accelerated reduction of air pollutants in China, 2017–2020 *Sci. Total Environ.* **803** 150011

Li H, Zheng B, Lei Y, Hauglustaine D, Chen C, Lin X, Zhang Y, Zhang Q and He K 2024 Trends and drivers of anthropogenic NO_x emissions in China since 2020 *Environ. Sci. Ecotechnol.* **21** 100425

Li K, Jacob D J, Liao H, Qiu Y, Shen L, Zhai S, Bates K H, Sulprizio M P, Song S and Lu X 2021a Ozone pollution in the North China plain spreading into the late-winter haze season *Proc. Natl Acad. Sci.* **118** e2015797118

Li M, Wu Y, Bao Y, Liu B and Petropoulos G P 2022b Near-surface NO_2 concentration estimation by random forest modeling and sentinel-5P and ancillary data *Remote Sens.* **14** 3612

Li S, Liu R, Wang S and Chen S X 2021b Radiative effects of particular matters on ozone pollution in six North China Cities *J. Geophys. Res. Atmos.* **126** e2021JD035963

Lin C, Lau A K, Fung J C, Song Y, Li Y, Tao M, Lu X, Ma J and Lao X Q 2021 Removing the effects of meteorological factors on changes in nitrogen dioxide and ozone concentrations in China from 2013 to 2020 *Sci. Total Environ.* **793** 148575

Liu F, Beirle S, Zhang Q, Van Der A R J, Zheng B, Tong D and He K 2017 NO_x emission trends over Chinese cities estimated from OMI observations during 2005–2015 *Atmos. Chem. Phys.* **17** 9261–75

Liu F, Page A, Strode S A, Yoshida Y, Choi S, Zheng B, Lamsal L N, Li C, Krotkov N A and Eskes H 2020 Abrupt decline in tropospheric nitrogen dioxide over China after the outbreak of COVID-19 *Sci. Adv.* **6** eabc2992

Liu M, Lin J, Wang Y, Sun Y, Zheng B, Shao J, Chen L, Zheng Y, Chen J and Fu T-M 2018 Spatiotemporal variability of NO_2 and $PM_{2.5}$ over Eastern China: observational and model analyses with a novel statistical method *Atmos. Chem. Phys.* **18** 12933–52

Murray C J, Aravkin A Y, Zheng P, Abbafati C, Abbas K M, Abbasi-Kangevari M, Abd-Allah F, Abdelalim A, Abdollahi M and Abdollahpour I 2020 Global burden of 87 risk factors in 204 countries and territories, 1990–2019: a systematic analysis for the Global Burden of Disease Study 2019 *Lancet* **396** 1223–49

Qian Z, Meng Q, Chen K, Zhang Z, Liang H, Yang H, Huang X, Zhong W, Zhang Y and Wei Z 2023 Machine learning explains long-term trend and health risk of air pollution during 2015–2022 in a Coastal City in Eastern China *Toxics* **11** 481

Schatke M, Meier F, Schröder B and Weber S 2022 Impact of the 2020 COVID-19 lockdown on NO_2 and PM_{10} concentrations in Berlin, Germany *Atmos. Environ.* **290** 119372

Shah V, Jacob D J, Li K, Silvern R F, Zhai S, Liu M, Lin J and Zhang Q 2020 Effect of changing NO_x lifetime on the seasonality and long-term trends of satellite-observed tropospheric NO_2 columns over China *Atmos. Chem. Phys.* **20** 1483–95

Shen Y, Jiang F, Feng S, Xia Z, Zheng Y, Lyu X, Zhang L and Lou C 2023 Increased diurnal difference of NO_2 concentrations and its impact on recent ozone pollution in eastern China in summer *Sci. Total Environ.* **858** 159767

Shen Y, Jiang F, Feng S, Zheng Y, Cai Z and Lyu X 2021 Impact of weather and emission changes on NO_2 concentrations in China during 2014–2019 *Environ. Pollut.* **269** 116163

Shi Z, Song C, Liu B, Lu G, Xu J, Van Vu T, Elliott R J, Li W, Bloss W J and Harrison R M 2021 Abrupt but smaller than expected changes in surface air quality attributable to COVID-19 lockdowns *Sci. Adv.* **7** eabd6696

Sun Z, Yang L, Bai X, Du W, Shen G, Fei J, Wang Y, Chen A, Chen Y and Zhao M 2019 Maternal ambient air pollution exposure with spatial-temporal variations and preterm birth risk assessment during 2013–2017 in Zhejiang Province, China *Environ. Int.* **133** 105242

Wang W, Li X, Cheng Y, Parrish D D, Ni R, Tan Z, Liu Y, Lu S, Wu Y and Chen S 2024 Ozone pollution mitigation strategy informed by long-term trends of atmospheric oxidation capacity *Nat. Geosci.* **17** 20–25

Wei J *et al* 2022 Ground-level NO_2 surveillance from space across China for high resolution using interpretable spatiotemporally weighted artificial intelligence *Environ. Sci. Technol.* **56** 9988–98

WHO 2021 Billions of people still breathe unhealthy air: new WHO data, edited

Xu R, Ye T, Yue X, Yang Z, Yu W, Zhang Y, Bell M L, Morawska L, Yu P and Zhang Y 2023 Global population exposure to

landscape fire air pollution from 2000 to 2019 *Nature* **621** 521–9

Xue T, Tong M, Wang M, Yang X, Wang Y, Lin H, Liu H, Li J, Huang C and Meng X 2023 Health impacts of long-term NO_2 exposure and inequalities among the Chinese population from 2013 to 2020 *Environ. Sci. Technol.* **57** 5349–57

Yang J, Wen Y, Wang Y, Zhang S, Pinto J P, Pennington E A, Wang Z, Wu Y, Sander S P and Jiang J H 2021 From COVID-19 to future electrification: assessing traffic impacts on air quality by a machine-learning model *Proc. Natl Acad. Sci.* **118** e2102705118

Zhao Y, Zhang K, Xu X, Shen H, Zhu X, Zhang Y, Hu Y and Shen G 2020 Substantial changes in nitrogen dioxide and ozone after excluding meteorological impacts during the COVID-19 outbreak in mainland China *Environ. Sci. Technol. Lett.* **7** 402–8